nature immunology

Mycobacterium tuberculosis blocks crosslinking of annexin-1 and apoptotic envelope formation on infected macrophages to maintain virulence

Huixian Gan[1], Jinhee Lee[2], Fucheng Ren[2], Minjian Chen[1], Hardy Kornfeld[2] & Heinz G Remold[1]

Macrophages infected with attenuated *Mycobacterium tuberculosis* strain H37Ra become apoptotic, which limits bacterial replication and facilitates antigen presentation. Here we demonstrate that cells infected with H37Ra became apoptotic after the formation of an apoptotic envelope on their surface was complete. This process required exposure of phosphatidylserine on the cell surface, followed by deposition of the phospholipid-binding protein annexin-1 and then transglutaminase-mediated crosslinking of annexin-1 through its amino-terminal domain. In macrophages infected with the virulent strain H37Rv, in contrast, the amino-terminal domain of annexin-1 was removed by proteolysis, thus preventing completion of the apoptotic envelope, which resulted in macrophage death by necrosis. Virulent *M. tuberculosis* therefore avoids the host defense system by blocking formation of the apoptotic envelope, which leads to macrophage necrosis and dissemination of infection in the lung.

Mycobacterium tuberculosis (Mtb), the causative agent of tuberculosis, infects alveolar macrophages, which provide a niche for the intracellular replication essential for the establishment of host infection[1]. Inhibition of phagosomal acidification and lysosome fusion enable intracellular parasitism by Mtb[2]. Apoptosis, a cell death modality that keeps the cell membrane barrier intact, is a common host-defense strategy against intracellular infection. Attenuated Mtb complex strains (H37Ra and *Mycobacterium bovis* bacille Calmette-Guerin) induce innate macrophage apoptosis at low multiplicity of infection (MOI)[3,4]. In contrast, virulent Mtb strains suppress that response and instead induce cell lysis and death in a process called 'necrosis'[4–8]. Apoptosis contributes to the host defense against tuberculosis by removing the intracellular macrophage niche by promoting microbicidal activity in macrophages[3,4,9] and by 'packaging' mycobacterial antigens in apoptotic vesicles that enhance presentation by dendritic cells[10,11]. In contrast, virulent Mtb strains activate necrosis, allowing viable bacilli to escape from host cells, after which they can infect new cells[12–14].

Although the early events of apoptosis have been studied extensively, the terminal steps required to complete apoptosis have received little attention. Among dying cells, a notable feature of those classified as 'apoptotic' is the presence of an impermeable cell membrane barrier on their outer surface called the 'apoptotic envelope'[15]. In terms of the host defense and responses to apoptotic cells, unique apoptotic envelope surface determinants signal uptake by phagocytes and convey anti-inflammatory signals[16], and the process of apoptosis confines bacilli in membranous vesicles 'marked' for engulfment by recruited phagocytes. In contrast, macrophage necrosis releases viable bacilli for extracellular spread of infection[17] and elicits inflammation, which contributes to tissue injury and the recruitment of naive macrophages that serve as hosts for subsequent rounds of infection. The detrimental effect of macrophage necrosis on tuberculosis defense *in vivo* has been demonstrated in studies of the genetic basis of tuberculosis susceptibility in mice[18].

In this study we addressed the mechanism of the formation of apoptotic envelopes in Mtb-infected cells, an underappreciated but critical terminal event for Mtb-infected macrophages. Formation of the apoptotic envelope involved defined variables including 'flopping' of phosphatidylserine, externalization of annexin-1 and crosslinking of annexin-1 by tissue transglutaminase (tTG). Virulent necrosis-inducing Mtb strains opposed this process by inducing proteolytic truncation of annexin-1 to a form that cannot be crosslinked. In macrophages infected with attenuated Mtb strains, annexin-1 truncation was inhibited by the serine-protease inhibitor PAI2 (plasminogen activator inhibitor type 2; also called SerpB2), which diminished the protease activity of tTG. Our data support a model that explains the divergent outcomes of Mtb-induced macrophage apoptosis or necrosis after infection with virulent or attenuated bacilli *in vitro* and *in vivo*.

RESULTS

Annexin-1 and PAI2 high-molecular-weight complexes

We hypothesized that surface exposure of phosphatidylserine on macrophages undergoing apoptosis after infection with the attenuated Mtb strain H37Ra provides binding sites for phosphatidylserine-binding

[1]Brigham & Women's Hospital and Harvard Medical School, Boston, Massachusetts, 02115, USA. [2]Department of Medicine, University of Massachusetts Medical School, Worcester, Massachusetts 01655, USA. Correspondence should be addressed to H.G.R. (hremold@rics.bwh.harvard.edu).

Received 22 July; accepted 14 August; published online 14 September 2008; doi:10.1038/ni.1654

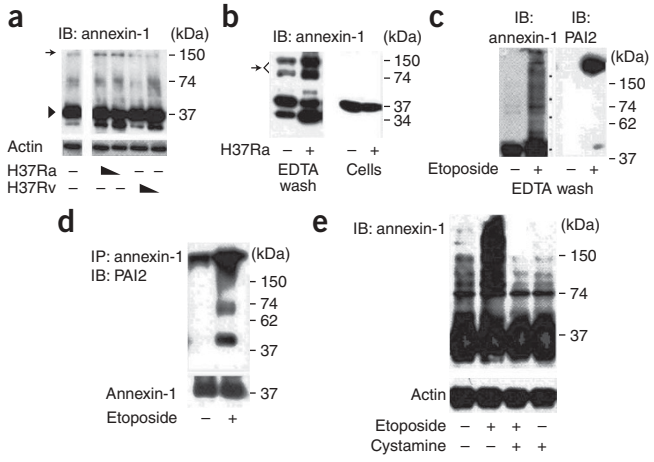

Figure 1 Macrophages undergoing apoptosis form a surface matrix containing crosslinked annexin-1 and PAI2. (**a**) Immunoblot analysis (IB) of annexin-1 and actin in lysates of human macrophages infected for 48 h with Mtb strain H37Ra, undergoing apoptosis, or strain H37Rv, undergoing necrosis (MOI, 5 and 2 (wedges)). Arrow indicates high-molecular-weight annexin-1; arrowhead indicates annexin-1. (**b**) Immunoblot analysis of annexin-1 in EDTA washes and lysates of macrophages left uninfected (–) or infected with H37Ra (+; MOI, 10), then surface-extracted with 2 mM EDTA in PBS. Arrow indicates high-molecular-weight annexin-1. (**c**,**d**) Immunoassay of RAW 264.7 cells treated for 48 h with 5 μM etoposide (+) or control medium (–) and then extracted with EDTA and analyzed by immunoblot for annexin-1 and PAI2 (**c**) or immunoprecipitated (IP) with anti-annexin-1 and analyzed by immunoblot for PAI2 or annexin-1 (below; loading control; **d**). (**e**) Immunoblot of annexin-1 and actin in lysates of RAW 264.7 cells treated with etoposide or control medium in the presence or absence of cystamine. Results are from one experiment of three.

proteins that are crosslinked into the developing apoptotic envelope. A search for candidate proteins containing phosphatidylserine-binding and crosslinking domains has identified annexin-1, a 37-kilodalton (37-kDa) protein[19,20] present in abundance on the surfaces of macrophages infected with attenuated rather than virulent Mtb[13]. Another candidate for crosslinking is PAI2, which is produced by many cell types, including macrophages[21].

If monomeric 37-kDa annexin-1 is crosslinked into the apoptotic envelope matrix, then it should be present in high-molecular-weight protein complexes. Lysates of macrophages undergoing apoptosis after infection with H37Ra contained annexin-1 complexes of over 150 kDa detectable by immunoblot analysis (**Fig. 1a**, arrow). Of note, uninfected macrophages and other cells[22] often have some discrete patches of annexin-1 on the cell surface. In contrast, the formation of high-molecular-weight annexin-1 complexes was much lower in macrophages infected with the virulent Mtb strain H37Rv, which led to necrosis. These findings established a correlation between high-molecular-weight annexin-1 and apoptosis.

We next investigated whether high-molecular-weight annexin-1 complexes accumulated on the surface of H37Ra-infected macrophages by taking advantage of the fact that binding of annexin-1 to cell membranes is Ca^{2+} dependent[19,23]. EDTA washes of H37Ra-infected macrophages contained two prominent high-molecular-weight annexin-1 complexes in greater abundance than those of EDTA washes from uninfected macrophages (**Fig. 1b**, arrow). Apoptosis therefore correlates with more formation of a surface matrix containing annexin-1 polymerized into high-molecular-weight complexes. Immunoblot analysis of the cells after EDTA extraction (**Fig. 1b**, cells) showed only the presence of 37-kDa annexin-1, which suggests that annexin-1 polymerization occurs on the cell surface.

To better synchronize the induction of apoptosis for biochemical studies and to evaluate annexin-1 crosslinking in a different context of apoptosis, we treated RAW 264.7 mouse macrophages with the apoptosis inducer etoposide[24]. We analyzed EDTA washes of control and etoposide-treated RAW 264.7 cells by immunoblot for annexin-1 and for PAI2 (**Fig. 1c**). EDTA-extractable material from apoptotic cell surfaces representing less than 2% of the total cell protein contained much more annexin-1 complexes of high molecular mass than did extracts from untreated control cells. PAI2 was also present in EDTA washes of apoptotic RAW 264.7 cells in a complex of over 175 kDa but was not detectable in washes of untreated cells (**Fig. 1c**). We immunoprecipitated lysates of RAW 264.7 cells with antibody to annexin-1 (anti- annexin-1) and analyzed the immunoprecipitates by immunoblot with anti-PAI2 (**Fig. 1d**). A large amount of PAI2-containing complexes, including many complexes of higher molecular weight, a component of about 74 kDa and the 47-kDa PAI2 monomer, was present in anti-annexin-1 precipitates of apoptotic RAW 264.7 cells. We detected only a small amount of the molecular PAI2 species of about 175 kDa in untreated cells. These findings indicated that PAI2 is incorporated into a high-molecular-weight matrix in apoptotic RAW 264.7 cells. The accumulation of high-molecular-weight annexin-1 complexes in RAW 264.7 cells was blocked by the tTG inhibitor cystamine[25] (**Fig. 1e**), which suggests that tTG-mediated protein crosslinking is required for formation of the apoptotic envelope.

Formation of the apoptotic envelope requires annexin-1

The experiments reported above showed that annexin-1 is a component of the high-molecular-weight surface matrix of macrophages undergoing apoptosis after Mtb infection or etoposide treatment, but did not clarify whether annexin-1 is a chief essential constituent of the apoptotic envelope. Studies of synthetic lipid vesicles have shown that phosphatidylserine is required for optimal annexin-1 polymerization[26], which suggests that the formation of two-dimensionally-ordered annexin-1 arrays in planar lipid bilayers facilitates tTG catalyzed crosslinking[27]. We propose that annexin-1 is spatially organized on the surface of apoptotic macrophages through its ability to bind phosphatidylserine, forming a template required for optimal crosslinking. Consequently, we targeted annexin-1 mRNA by RNA-mediated interference using small interfering RNA (siRNA) in RAW 264.7 cells to test whether lower annexin-1 production would result in more necrosis of etoposide-treated cells (**Supplementary Fig. 1a** online). In contrast to vector-treated cells or cells treated with nontargeting siRNA, cells targeted for annexin-1 silencing underwent rapid necrosis after etoposide treatment (**Fig. 2a**). These data indicated that full-length annexin-1 is essential for the formation of a stable apoptotic envelope and that the apoptotic cell death mode initiated by etoposide treatment proceeds to necrosis in the absence of annexin-1.

PAI2, which is incorporated into the high-molecular-weight matrix of apoptotic macrophages, belongs to a group of protease inhibitors that protect cells against injury and mycobacteria-induced death[28,29]. To evaluate the function of PAI2 in the formation of apoptotic envelopes, we used the cyclooxygenase inhibitor indomethacin to inhibit PAI2 synthesis in human macrophages and RAW 264.7 cells[29,30] (**Supplementary Fig. 1b**,**c**). To exclude the possibility of unrelated effects of indomethacin, we also tested macrophages from PAI2-deficient mice. Infection with H37Ra induced apoptosis but little necrosis in untreated human or wild-type mouse macrophages. In contrast, H37Ra infection of indomethacin-treated macrophages or of

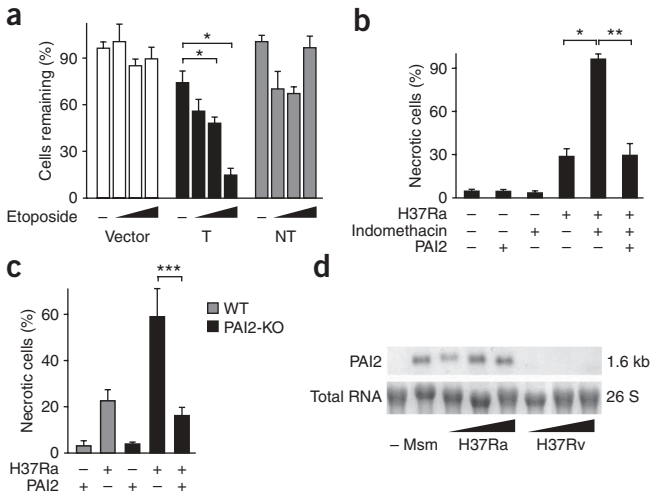

Figure 2 'Silencing' of annexin-1 abrogates formation of the apoptotic envelope. (**a**) Spectrophotometry of viable RAW 264.7 cells preincubated with vector alone (Vector), siRNA targeting annexin-1 (T) or nontargeting siRNA (NT), then treated for 48 h with 0 μM (–) or 1, 5 or 10 μM (wedges) etoposide and stained with the vital dye MTT. *, $P = 0.002$. (**b**,**c**) Fluorescence microscopy of necrotic human macrophages infected for 96 h with H37Ra (MOI, 10) in the presence or absence of indomethacin and/or recombinant PAI2 (**b**) or wild-type and PAI2-deficient mouse macrophages infected for 96 h with H37Ra (MOI, 10) without or with recombinant PAI2 (100 μg/ml; **c**), then stained with propidium iodide and counted at a magnification of ×100, presented as mean percent necrotic macrophages. *, $P = 0.07$; **, $P = 0.004$; ***, $P = 0.002$. (**d**) RNA blot analysis of the expression of PAI2 mRNA and 26S ribosomal RNA in human macrophages infected for 24 h with *M. smegmatis* (Msm), or for 10 h with H37Ra or H37Rv. Data are representative of six (**a**), four (**b**) or three (**c**) experiments (error bars, s.e.m.) or are from one representative of four experiments with similar results (**d**).

PAI2-deficient mouse macrophages resulted in necrosis (**Fig. 2b**,**c** and **Supplementary Fig. 2** online). The addition of recombinant PAI2 to PAI2-depleted or PAI2-deficient macrophage cultures prevented necrosis. Exogenous recombinant PAI2 alone had no effect on apoptosis, as detected by *in situ* TUNEL assay of cell death (31% ± 4% for indomethacin-treated cells infected with H37Ra for 48 h versus 37% ± 4% for indomethacin- and PAI2-treated cells infected with H37Ra; $n = 3$ experiments; $P = 0.36$). Lower PAI2 production might contribute to the necrosis of macrophages infected with virulent Mtb, as H37Rv did not induce PAI2 mRNA accumulation, whereas H37Ra-infected macrophages had high expression of this mRNA (**Fig. 2d**).

Cleavage of annexin-1 by virulent Mtb

The finding that PAI2 protected the completion of apoptosis and prevented necrosis suggested that it inhibits the proteolysis of proteins involved in generating the macrophage surface-associated high-molecular-weight protein matrix. We postulate that 37-kDa annexin-1 is essential for matrix formation because it binds to phosphatidylserine and is a substrate for crosslinking by tTG[26]. The amino-terminal annexin-1 domain contains glutamine residues available for crosslinking at positions 10, 19 and 23 (ref. 23). Proteolytic excision of this domain results in a 34-kDa annexin-1 that cannot be crosslinked[26] yet binds phosphatidylserine on the cell surface more avidly than 37-kDa annexin-1 does[23]. We therefore investigated whether PAI2 inhibits annexin-1 proteolysis (**Fig. 3**). Infection of macrophages with H37Rv resulted in much more cleavage of annexin-1 to the 34-kDa fragment than did infection with H37Ra (**Fig. 3a**). Depletion of endogenous PAI2 with indomethacin increased the amount of cleaved 34-kDa annexin-1 in H37Ra-infected macrophages, and this effect was blocked by the addition of recombinant PAI2 (**Fig. 3b**). Proteolysis of the 37-kDa annexin-1 in H37Rv-infected macrophages was inhibited by exogenous recombinant PAI2 (**Fig. 3c**). These findings suggest that greater proteolytic cleavage of annexin-1 in H37Rv-infected macrophages is a consequence of less synthesis of PAI2.

Lipopolysaccharide (LPS) induces PAI2 production by enhancing transcription of the gene encoding PAI2 and by increasing the half-life of the PAI2 transcripts[31]. To determine whether LPS-induced PAI2 mRNA accumulation was affected by Mtb, we incubated macrophages with LPS and infected the cells with H37Rv. H37Rv abrogated the LPS-induced accumulation of PAI2 mRNA (**Fig. 4a**), which suggests that an active process inhibits this event. In contrast, inoculation with the attenuated H37Ra did not downregulate LPS-induced PAI2 mRNA (data not shown). Large amounts of lipoxin A_4 (LXA_4), an anti-inflammatory eicosanoid[32], correlate with greater susceptibility to Mtb infection[33]. We therefore measured LXA_4 and found its concentration was higher in H37Rv-infected macrophages than in H37Ra-infected macrophages (**Fig. 4b**), which suggests involvement of LXA_4 in suppression of PAI2 synthesis. Indeed, exogenous LXA_4 significantly inhibited PAI2 expression in H37Ra-infected macrophages (**Fig. 4c**). These experiments identify LXA_4 produced by H37Rv-infected macrophages as an important downregulator of PAI2 production that leads to more proteolytic cleavage of 37-kDa annexin-1 and necrosis.

Etoposide treatment of RAW 264.7 cells induced PAI2 production in a cyclooxygenase-dependent way similar to that of primary human macrophages infected with H37Ra (**Supplementary Fig. 1b**,**c**). Incubation of etoposide-treated RAW 264.7 cells with indomethacin caused necrosis that was reversed by exogenous recombinant PAI2 (**Supplementary Fig. 3a** online), whereas recombinant PAI2 did not alter the number of $TUNEL^+$ cells (36 ± 7% versus 35 ± 12%; $n = 5$ experiments; $P = 0.9$). Proteolysis of annexin-1 was much higher in RAW 264.7 cells treated with indomethacin plus etoposide. This correlated with enhanced necrosis (release of lactate dehydrogenase because of plasma membrane lysis) and was inhibited by the addition of recombinant PAI2 (**Supplementary Fig. 3b**,**c**). These data indicate

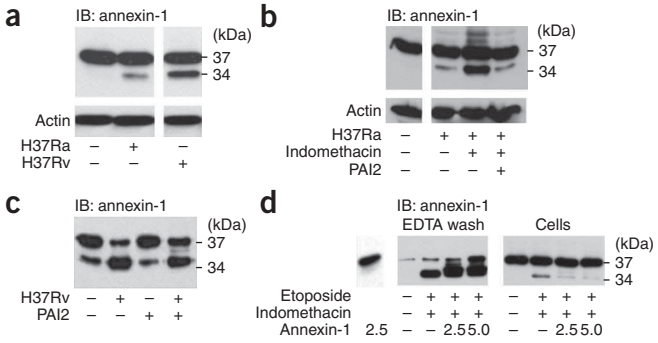

Figure 3 Annexin-1 cleavage is regulated by PAI2. (**a**–**c**) Immunoblot analysis of annexin-1 and actin in human macrophages infected for 48 h with H37Rv (MOI, 10; **a**,**c**) or H37Ra (**a**,**b**) without (**a**) or with (**b**,**c**) indomethacin (50 μg/ml) and/or recombinant PAI2 (100 μg/ml). (**d**) Immunoblot analysis of annexin-1 in EDTA washes and cell extracts of RAW 264.7 cells treated with etoposide, indomethacin and/or recombinant or annexin-1 (2.5 or 5 μg/ml). Actin staining confirms equal loading of lanes (data not shown). Results are from one of three experiments.

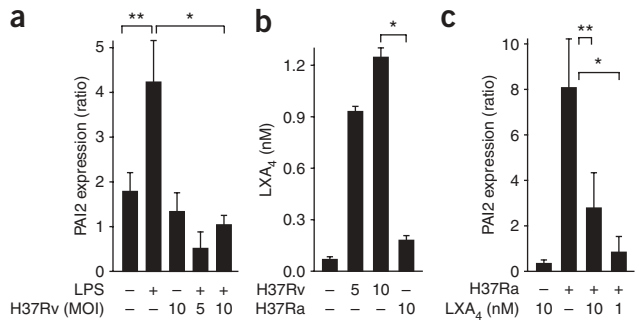

Figure 4 Effect of virulent H37Rv on the accumulation of PAI2 mRNA. (**a**) RT-PCR of PAI2 mRNA in macrophages (5×10^5 per plate) cultured with (+) or without (–) LPS (10 ng/ml) and infected for 24 h with H37Rv at an MOI of 5 or 10, presented as the ratio of PAI2 mRNA to actin mRNA ('fold difference'). *, $P = 0.05$; **, $P = 0.01$. (**b**) Induction of LXA_4 by culture of macrophages with H37Ra or H37Rv (MOI, 5 or 10), measured in supernatants after 12 h. *, $P = 0.001$. (**c**) RT-PCR of PAI2 mRNA in macrophages left uninfected (–) or infected for 24 h with H37Ra (MOI, 10) in the presence or absence of LXA_4 (concentrations, below graph), presented as described in **a**. *, $P = 0.001$; **, $P = 0.03$. Data are representative of four (**a**) or three (**b**,**c**) experiments (error bars, s.e.m.).

that annexin-1 cleavage in RAW 264.7 cells correlates with secondary necrosis due to accumulation of a 34-kDa annexin-1 fragment that cannot be crosslinked.

Cleavage of annexin-1 on or near the macrophage surface

Our findings reported above (**Fig. 1b**) suggested that annexin-1 cleavage occurs at the macrophage surface. To investigate this further, we treated PAI2-depleted RAW 264.7 cells for 24 h with etoposide after adding full-length recombinant annexin-1. We analyzed EDTA washes and the corresponding cytosolic lysates by immunoblot with anti-annexin-1 (**Fig. 3d**). The EDTA wash of PAI2-depleted cells contained mainly the 34-kDa annexin-1 fragment. The addition of 37-kDa recombinant annexin-1 increased the 34-kDa annexin-1 fragment only in the EDTA washes and not in the cytosolic fractions. Only 37-kDa annexin-1 was present in the cytosol, and its amount was similar whether recombinant annexin-1 was added to the cells or not. These experiments confirmed that cleavage of annexin-1 to the 34-kDa fragment occurs on or near the cell surface.

To further evaluate the association of annexin-1 with the apoptotic envelope, we did fluorescence microscopy and flow cytometry of primary human macrophages and RAW 264.7 cells made permeable with digitonin for intracellular staining. For this, we used antibodies to 37-kDa annexin-1, which do not detect the 34-kDa annexin-1 fragment. Full-length 37-kDa annexin-1 accumulated on the surface of H37Ra-infected human macrophages and to a smaller extent on untreated macrophages (**Fig. 5a**, left and center, and **Supplementary Fig. 4** online) but was not detected on the surface of necrotic macrophages (**Fig. 5a**, right). Apoptosis of etoposide-treated RAW 264.7 cells was also associated with the accumulation of 37-kDa annexin-1 on the cell surface (**Fig. 5b**,**c**). In contrast, the 37-kDa annexin-1 did not accumulate on the surface of RAW 264.7 cells depleted of PAI2 with indomethacin and treated with etoposide (**Fig. 5b**,**c**) and was diffusely distributed in the cell. This indicates that in necrotic RAW 264.7 cells, 37-kDa annexin-1 is not transported to the cell surface or is immediately cleaved after arrival on the cell surface[34].

To investigate whether proteolysis of 37-kDa annexin-1 inhibits its incorporation into the high-molecular-weight matrix, we depleted primary macrophages and RAW 264.7 cells of PAI2 and either infected them with H37Ra or treated them with etoposide for 24 h. Immunoblot analysis of EDTA-extractable annexin-1 demonstrated that PAI2-depleted, H37Ra-infected macrophages had much less high-molecular-weight annexin-1–positive complex (**Fig. 5d**). Likewise, PAI2-depleted RAW 264.7 cells treated with etoposide had little high-molecular-weight annexin-1, as did untreated controls (**Fig. 5e**). Reconstitution with recombinant PAI2 restored formation of the high-molecular-weight matrix. These data support the hypothesis that crosslinked 37-kDa annexin-1 forms the high-molecular-weight

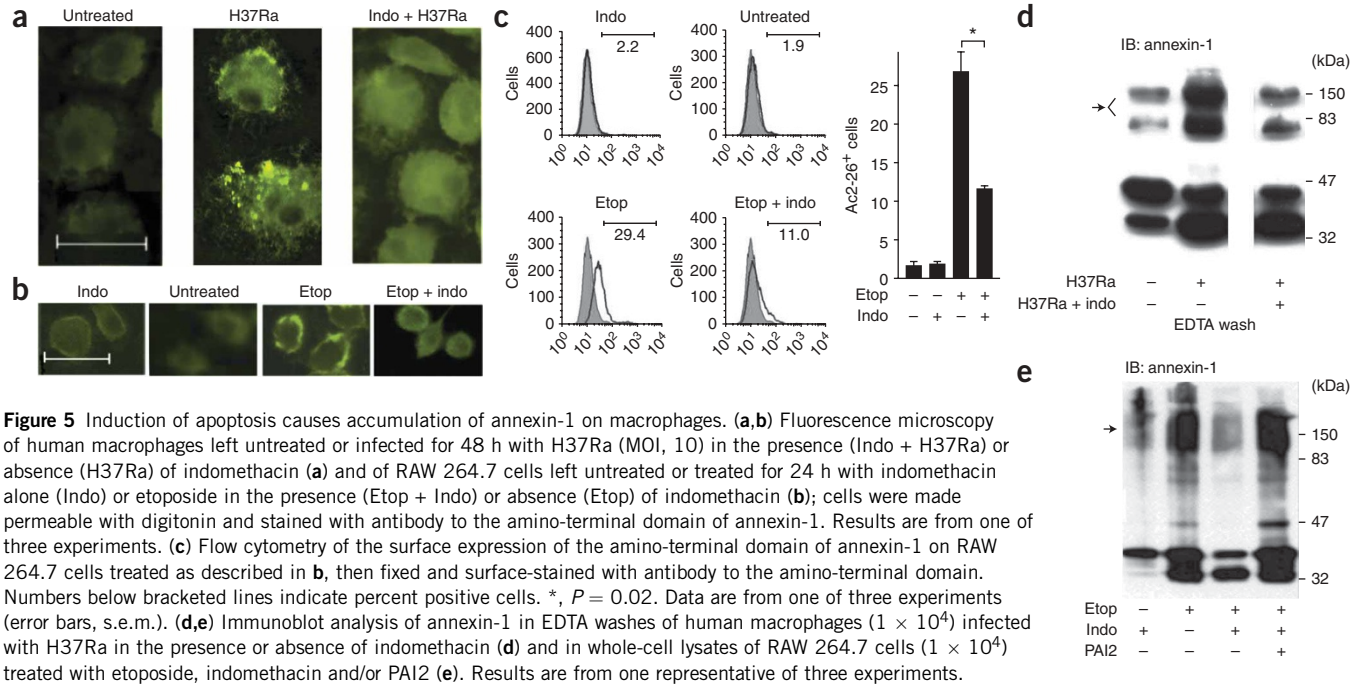

Figure 5 Induction of apoptosis causes accumulation of annexin-1 on macrophages. (**a**,**b**) Fluorescence microscopy of human macrophages left untreated or infected for 48 h with H37Ra (MOI, 10) in the presence (Indo + H37Ra) or absence (H37Ra) of indomethacin (**a**) and of RAW 264.7 cells left untreated or treated for 24 h with indomethacin alone (Indo) or etoposide in the presence (Etop + Indo) or absence (Etop) of indomethacin (**b**); cells were made permeable with digitonin and stained with antibody to the amino-terminal domain of annexin-1. Results are from one of three experiments. (**c**) Flow cytometry of the surface expression of the amino-terminal domain of annexin-1 on RAW 264.7 cells treated as described in **b**, then fixed and surface-stained with antibody to the amino-terminal domain. Numbers below bracketed lines indicate percent positive cells. *, $P = 0.02$. Data are from one of three experiments (error bars, s.e.m.). (**d**,**e**) Immunoblot analysis of annexin-1 in EDTA washes of human macrophages (1×10^4) infected with H37Ra in the presence or absence of indomethacin (**d**) and in whole-cell lysates of RAW 264.7 cells (1×10^4) treated with etoposide, indomethacin and/or PAI2 (**e**). Results are from one representative of three experiments.

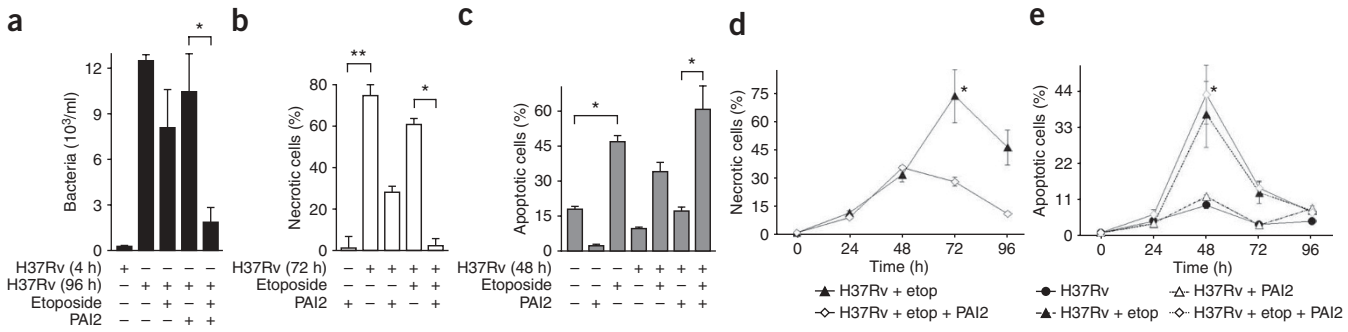

Figure 6 PAI2 protects against macrophage necrosis and contributes to antimycobacterial activity in human macrophages infected with H37Rv. Analysis of the bacterial burden (**a**) and necrosis or apoptosis (**b**–**e**) of macrophages infected with H37Rv (MOI, 10; time, below graphs) and treated with various combinations of etoposide and PAI2. (**a**) Bacterial burden at 96 h. *, $P = 0.001$. (**b**) Flow cytometry of necrotic (propidium iodide–positive) cells at 72 h. *, $P < 0.007$; **, $P = 0.0001$. (**c**) TUNEL staining for apoptosis at 48 h. *, $P = 0.015$. (**d**,**e**) ELISA photometric enzyme immunoassay of necrosis (**d**) and apoptosis (**e**) at 0–96 h after infection. (**d**) *, $P = 0.001$, 72 and 96 h. (**e**) *, $P = 0.003$. Data are representative of six (**a**) or five (**b**,**c**) experiments or are from one of three experiments (**d**,**e**; error bars (**a**–**e**), s.em.).

matrix that is characteristic of the macrophage apoptotic envelope and that annexin-1 cleavage prevents formation of the apoptotic envelope.

Antimycobacterial PAI2 activity blocks necrosis

It has been shown before that necrotic macrophages do not compromise the viability of the bacilli[12,14]. Because PAI2 seemed to be involved in macrophage apoptosis, we investigated whether it promotes antimycobacterial activity. Consistent with our findings, H37Rv replicated over time in infected human macrophages. In presence of etoposide, intracellular H37Rv replication was not diminished. However, when PAI2 was added, etoposide significantly diminished the Mtb burden (**Fig. 6a**). To understand the function of different death modalities in the decrease in the H37Rv burden, we measured macrophage necrosis and apoptosis. H37Rv induced necrosis in macrophages that was prevented by the addition of exogenous recombinant PAI2 in presence of etoposide (**Fig. 6b–e**). Moreover, apoptosis was also induced in cultures of H37Rv-infected macrophages treated with etoposide alone or with recombinant PAI2 and etoposide together (**Fig. 6c,e**). PAI2 was not involved in the induction of apoptosis, as there was no significant difference in the apoptosis of macrophage cultures treated with H37Rv and etoposide and those treated with H37Rv, etoposide and PAI2 (**Fig. 6c,e**). We concluded that PAI2 allows less H37Rv growth by preventing macrophage necrosis.

The serpin PAI2 has a 33–amino acid C-D interhelical loop that contains glutamine residues at positions 83, 84 and 86 (ref. 35), which makes it a potential substrate for tTG-mediated crosslinking. Crosslinked PAI2 is found in trophoblast membranes and in the corneal envelope of keratinocytes[15,21,36], and we found that PAI2 was part of the surface matrix of apoptotic RAW 264.7 cells (**Fig. 1**). Native PAI2 protects HeLa cells from death induced by tumor necrosis factor, whereas PAI2 lacking the C-D interhelical loop is not protective[37]. We therefore investigated whether PAI2 crosslinking was required for formation of the macrophage apoptotic envelope. We compared the ability of the following forms of PAI2 to protect PAI2-depleted RAW 264.7 cells from etoposide-induced necrosis: native PAI2; a PAI2 mutant lacking the C-D interhelical domain but able to interact with urokinase-type plasminogen activator (uPA); and a PAI2 mutant with the P1 reactive-center arginine at position 380, needed for protease inhibition, replaced with alanine (**Supplementary Fig. 5** online). The mutant with a substitution in the P1 reactive center did not prevent necrosis, which indicated that protease inhibition is required for the antinecrotic activity of PAI2. In contrast, ablation of the C-D interhelical loop did not alter the ability of PAI2 to inhibit necrosis, which indicated that PAI2 crosslinking is not required for its antinecrotic activity. These data are confirmed by evidence that other protease inhibitors lacking an interhelical domain are able to block programmed cell death[38].

Inhibition of the apoptotic envelope correlates with more necrosis

To determine how the observed *in vitro* macrophage cytotoxicity difference between H37Ra and H37Rv relates to *in vivo* conditions, we challenged BALB/c mice with 1×10^5 colony-forming units of either Mtb strain by tracheal instillation and then compared cell populations in bronchoalveolar lavage (BAL) fluid 9 and 14 d later. At day 9 there were far more necrotic (propidium iodide–positive) macrophages in mice challenged with H37Rv than in those challenged with H37Ra (**Fig. 7a**). This difference persisted at day 14 (data not shown). We further analyzed cell populations in BAL fluid by flow

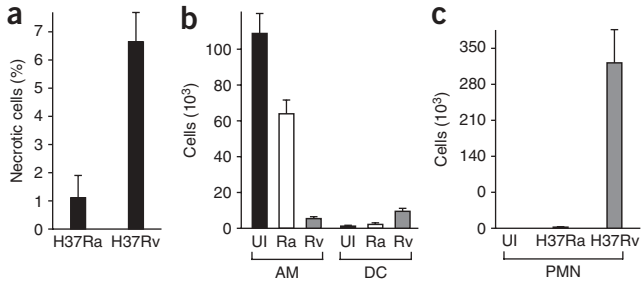

Figure 7 *In vivo* cytotoxicity of virulent Mtb. Analysis of cells in BAL fluid obtained 9 or 14 d after challenge of mice by tracheal instillation of 1×10^5 colony-forming units of H37Ra or H37Rv. (**a**) Necrosis of cells 9 d after infection, assessed by propidium iodide staining and presented as percent propidium iodide–positive cells. $P = 0.004$. Data are representative of four experiments (error bars, s.e.m.). (**b**) Flow cytometry and hemocytometry of resident alveolar macrophages (AM; $CD11b^{lo}CD11c^{hi}$) and lung myeloid dendritic cells (DC; $CD11b^{hi}CD11c^{hi}$) among total cells in BAL fluid on day 14 after infection. $P < 0.01$, infected resident alveolar macrophages, H37Rv (Rv) versus H37Ra (Ra); $P < 0.001$, lung myeloid dendritic cells, H37Rv versus control and H37Rv versus H37Ra. Data are representative of three experiments (error bars, s.e.m.). (**c**) Flow cytometry and hemocytometry of lung neutrophils (PMN; $CD11b^{+}Gr\text{-}1^{+}F4/80^{-}$) among total cells in BAL fluid on day 14 after infection. $P < 0.001$. Data are from one of three experiments (error bars, s.e.m.).

cytometry on day 14 after Mtb challenge by staining for the markers CD11b, CD11c, F4/80 and Gr-1. We found significant differences in the composition of lung leukocyte populations. Infection with H37Rv resulted in many fewer resident alveolar macrophages (defined as $CD11b^{lo}CD11c^{hi}$) than did H37Ra infection and or no infection (mean, 5,642 versus 63,798 and 109,203, respectively), whereas $CD11b^{hi}CD11c^{hi}$ myeloid dendritic cell numbers were higher only in H37Rv-infected mice (**Fig. 7b**). The airways of H37Rv-infected mice were repopulated with a large number of neutrophils (defined as $F4/80^{-}Gr\text{-}1^{+}$), in contrast to those of H37Ra-infected mice, in which neutrophils remained a negligible population (**Fig. 7c**). We confirmed the presence of many more neutrophils in the BAL fluid of H37Rv-infected mice than in the BAL fluid of control and H37Ra-infected mice by Giemsa staining (data not shown). These results suggest that the ability of H37Rv to promote macrophage necrosis through interference with formation of the apoptotic envelope contributes to disease manifestations unique to virulent bacilli *in vivo*, producing a proinflammatory necrotic milieu that considerably alters pulmonary leukocyte populations. To explain the formation of the apoptotic envelope, we propose the sequence of events outlined in **Supplementary Figure 6** online.

DISCUSSION

Mycobacertial virulence depends on the invasion of lung macrophages and inhibition of phagosome maturation to create a protected intracellular niche for bacterial replication. The ability of Mtb to survive in macrophages, even in face of interferon-γ activation, presents a challenge to host defense analogous to intracellular infection by viruses. One common strategy for dealing with this problem is to eliminate infected cells by apoptosis[39]. An innate tumor necrosis factor–mediated macrophage-apoptosis pathway triggered by bacille Calmette-Guerin or H37Ra at low MOI has been described[3,4,40], and mitochondrial membrane destabilization is also important in the induction of macrophage programmed cell death induced by Mtb[13].Other innate apoptosis pathways have been described[41,42], and apoptosis is also a chief outcome of the adaptive immune response to infected macrophages by means of signaling through the cell surface receptor Fas and the actions of granzymes[9,43]. In addition to eliminating the niche for mycobacterial replication, apoptosis creates an intracellular environment hostile to Mtb[3–5,9] and sequesters bacilli in apoptotic bodies that facilitate antigen presentation by dendritic cells[10,11] as well as engulfment and enhanced killing by newly recruited phagocytes[14,17].

Initial macrophage apoptosis is downregulated by virulent Mtb strains that promote macrophage necrosis, particularly at high intracellular bacillary loads[12,13]. Necrosis is detrimental to the host defense against tuberculosis. It releases viable intracellular bacilli for spreading infection and promotes tissue damage characteristic of advanced tuberculosis disease, a conclusion supported by published work that has identified a allele in mice linked to tuberculosis susceptibility that is associated with more necrosis of infected macrophages *in vitro* and giant necrotic lung lesions *in vivo*[18]. The outcome of tuberculosis disease seems to reflect the relative ability of the host to limit Mtb growth and spread by containment in apoptotic bodies versus the ability of the pathogen to grow intracellularly and then exit infected macrophages by inducing a death mode with predominant features of necrosis.

The initiation of apoptosis by Mtb has generated considerable interest, but 'downstream' events that culminate in the formation of the apoptotic envelope have not been considered. Here we have presented the new finding that macrophage apoptosis induced by attenuated H37Ra led to the formation of apoptotic envelopes by tTG-dependent crosslinking of annexin-1 and PAI2. Infection with virulent H37Rv was associated with cleavage of annexin-1 to a form that cannot be crosslinked. This prevented formation of the apoptotic envelope matrix and resulted in necrosis of the infected macrophages. We confirmed those findings in Mtb-infected primary macrophages of human and mouse origin and in RAW 264.7 cells and determined that crosslinking of annexin-1 was essential for formation of the apoptotic envelope in the very different context of etoposide-induced apoptosis. This indicates that our findings represent a general mechanism of apoptotic envelope formation.

We further showed by *in vivo* experiments that lack of apoptotic envelope formation correlated with rampant necrosis. In mice challenged by tracheal instillation of virulent H37Rv, significantly more necrotic cells were present in the lungs at day 9 after infection, which correlated with significant depletion of alveolar macrophages and was followed by a considerable influx of neutrophils[44]. Neutrophil influx is known to occur when massive necrotic events trigger the production of inflammatory chemokines[45].

We propose the following sequence of events leading to the formation of apoptotic envelopes in Mtb-infected macrophages. Infection triggers exposure of phosphatidylserine on the macrophage surface, followed by translocation of annexin-1 to the outer plasma membrane leaflet. Binding of annexin-1 to phosphatidylserine on the cell surface[46] arranges the annexin-1 in a two-dimensional array that facilitates crosslinking by tTG to form a stable apoptotic envelope[26]. However, 37-kDa annexin-1 deposited on the cell surface may be cleaved by endogenous proteases to the 34-kDa form that avidly binds phosphatidylserine but cannot be crosslinked by tTG. If crosslinking is not achieved, the apoptotic envelope matrix fails to form and the cell progresses to necrosis. The as-yet-unidentified endogenous protease involved in that reaction is inhibited by PAI2. Downregulation of PAI2 (as occurs after H37Rv infection) results in more accumulation of 34-kDa annexin-1, prevents apoptotic envelope formation and promotes cell membrane disintegration and necrosis. The differences between apoptosis and necrosis induced by attenuated and virulent Mtb are probably not absolute, as many cell-death pathways may be elicited, but our data have shown that competition between tTG-dependent crosslinking and proteolytic cleavage of annexin-1 on the macrophage surface may be a physiologically important equilibrium influenced by host and pathogen variables.

Studies of other systems corroborate our model. Apoptosis of rat liver cells, human epidermal cells and human lung cancer cells leads to synthesis of an SDS-insoluble polymer formed by tTG-mediated crosslinking of proteins including annexin-1 and PAI2 (refs. 15,21, 47–51). It has been shown that the plasminogen activator Pla, a surface proteinase produced by *Yersinia pestis*, is essential for the development of primary pneumonic plague, a usually lethal necrotizing lung infection, whereas it is not involved in the development of the bubonic form of plague[52]. We speculate that Pla processes annexin-1 into the truncated 34-kDa form, leading to massive necrosis and inflammation of the lung tissue.

The clade B serpin PAI2 inhibits uPA, which converts plasminogen to plasmin[53]. Most serpins are intracellular proteins; past studies of PAI2 have aimed mainly at identifying an intracellular function because of its inefficient signal sequence[54]. In contrast, our studies here have indicated that PAI2 acts on the cell surface to prevent proteolysis of annexin-1. PAI2 has a reactive side loop containing the P1-P1′ amino acid residues that interacts with the active-site serine of the target protease[55]. The P1 arginine at position 380 is required for inhibition of uPA activity and inhibition of cell death in other

systems[38]. A second attribute of PAI2 necessary for the inhibition of cell death is the 33–amino acid loop between helices C and D, which contains three glutamine residues necessary for crosslinking, which results in PAI2 that is copolymerized but functionally active[35–37]. In contrast to the previous findings[37], we found that PAI2 lacking the 33-residue amino acid loop was as active as native PAI2 in blocking the necrosis of macrophages undergoing etoposide-mediated apoptosis. PAI2 lacking the C-D interhelical loop binds to the active site of uPA, the true substrate for PAI2 (ref. 54), which forms a covalent complex and inactivates uPA as efficiently as native PAI2. Therefore, crosslinking of PAI2 into the apoptotic envelope is not required for protection of annexin-1 from proteolysis in *in vitro* conditions, although it remains possible that tethering the serpin to the nascent apoptotic envelope *in vivo* prevents its diffusion in limiting conditions.

Apoptosis and necrosis are increasingly recognized as exerting different influences on tuberculosis defense and pathogenesis. In general terms, necrosis is understood to occur after bioenergetic collapse[56] or as a unique regulated death mode called 'programmed necrosis'[57]. Our data have defined another pathway to necrosis caused by failure of the formation of a stable envelope matrix in macrophages undergoing apoptosis. Although much attention has been paid to the initiation of macrophage apoptosis by Mtb, the terminal events leading to the formation of stable apoptotic vesicles have not been explored before, to our knowledge. We have presented evidence here that crosslinking of 37-kDa annexin-1 was an essential step for the creation of apoptotic envelopes in Mtb-infected macrophages and that failure to protect full-length annexin-1 from cleavage to its 34-kDa form resulted in necrosis. The different regulation of PAI2 expression by H37Ra and H37Rv that we have described may account, at least in part, for the mainly necrotic death of macrophages infected with the latter. Our results have shown that focusing exclusively on early events in apoptosis, such as nuclear fragmentation, gives an incomplete picture of the death mode of macrophages infected with Mtb. Investigating the biochemistry and the functions of the apoptotic envelope will provide a better understanding of the mechanisms by which the host sequesters and kills intracellular pathogens and might identify new targets for drug development and new insights into vaccine development.

METHODS

Materials. The following reagents were used: fluorescein isothiocyanate–conjugated goat anti–rabbit immunoglobulin G conjugate (L42001) and polyclonal goat anti-rabbit, purified (L43000; both from Zymed); rabbit polyclonal anti-annexin-1 (072-13) and rabbit antibody to the amino-terminal human annexin-1 peptide Ac2-26 (H-07213; Phoenix Pharmaceuticals); anti-actin (JLA20) and anti–mouse annexin-1 (EH17a; Hybridoma Bank, The University of Iowa); allophycocyanin–Alexa Fluor 750–conjugated anti-CD11b (M1/70) and phycoerythrin-conjugated anti-F4/80 (BM8; eBiosciences); human purified recombinant annexin-1 (Biodesign); rabbit immunoglobulin G (Upstate); protease inhibitor 'cocktail' (Roche); HEPES and dithiothreitol (Invitrogen); and propidium iodide, MTT (3-(4,5-dimethylthiazol-2-yl)-2,5-diphenyl tetrazolium bromide) and LPS (Sigma).

Bacteria. Mtb H37Rv and H37Ra and *Mycobacterium smegmatis* (American Type Culture Collection) were grown as described[13] and were stored at –80 °C. Frozen stocks were thawed, sonicated for 10 s and then allowed to settle for 10 min. Clumps were dispersed by ten aspirations through a 29-gauge needle (Becton Dickinson).

Quantification of mycobacteria. Adherent macrophages were infected with H37Ra or H37Rv at an MOI of 2, 5 or 10. After 4 h, cells were washed five times with Hank's balanced-salt solution and were cultured in Iscove's modified Dulbecco's medium (Invitrogen). Mycobacterial growth was measured after cell lysis with 500 μl of 0.2% (wt/vol) SDS in PBS (neutralized with 500 μl of 50% (vol/vol) FCS), serial dilution of 100-μl cell lysates from triplicate cultures and plating on 7H10 agar plates (Remel). Colonies were counted after 21 d. Alternatively, 100-μl cell lysates were pooled and were inoculated into triplicate Bactec 12B vials (Bactec model 460TB; BD Biosciences).

Cells and culture. Mononuclear cells from buffy coat preparations (Research Blood Component)[13] were cultured for 7 d in Iscove's modified Dulbecco's medium containing 10% (vol/vol) human AB serum (Gemini) at a density of 2.0×10^6 cells per ml in six-well plates and then were challenged with Mtb. RAW 264.7 cells (American Type Culture Collection) were cultured in RPMI medium with 10% (vol/vol) FCS to a density of 2.0×10^6 cells per ml. For depletion of PAI2, 100 μM indomethacin was added to cells before the addition of 5 μM etoposide or Mtb. For reconstitution of PAI2, recombinant PAI2 (5 μg/ml) was added. Mice with deletion of the gene encoding PAI2 (ref. 58) were obtained from H.F. Rosenberg. Wild-type mice were from Jackson Laboratories. Of the mouse spleen macrophages isolated by adherence to plastic dishes, 95% were macrophages, as determined by nonspecific esterase stain and staining with anti-CD11b and anti-F4/80. Human studies were approved by the Partners Human Research Committee; mouse studies were approved by the Animal Care and Use Committee of the Dana-Farber Cancer Institute.

***In vitro* assays of apoptosis and necrosis.** Apoptosis of macrophages *in vitro* was assessed with a fluorescent *in situ* TUNEL assay according to the manufacturer's specifications (terminal deoxynucleotidyl transferase-mediated dUTP nick end-labeling; *In situ* Cell Death Detection Kit; TMR Red; Roche). For measurement of necrosis, primary macrophages cultures were treated for 10 min at 25 °C with propidium iodide (10 μg/ml in PBS), then coverslips were washed twice with PBS and examined with a fluorescence microscope. In some experiments, apoptosis and necrosis were measured with the cell death detection ELISA^{PLUS} photometric enzyme immunoassay (11 920685 001; Roche Applied Science) for the quantification of cytoplasmic (apoptosis) and extracellular (necrosis) histone-associated DNA fragments according to the specifications of the manufacturer. Necrosis of RAW 264.7 cells was determined by measurement of the concentration of L-lactate and NAD oxyreductase (lactate dehydrogenase; EC 1.1.1.27) in cell-free supernatants and lysates by ELISA, according to the specifications of the manufacturer (Sigma); by analysis of the number of remaining cells after culture for 4 h with MTT (0.8 mg/ml)[59] by measuring absorbance at 560 nm with a microplate spectrophotometer; and by flow cytometry with gating of 7-amino-actinomycin D–positive, annexin V–positive cells with the phycoerythrin-conjugated annexin V apoptosis detection kit (BD Biosciences Pharmingen).

LXA_4 assay. LXA_4 was assayed with an ELISA kit according to the recommendations of the manufacturer (Oxford Biomedical Research).

Determination and fluorescence imaging of 37-kDa cell surface annexin-1. The 37-kDa annexin-1 was assayed by flow cytometry. Human macrophages and RAW 264.7 cells (1×10^7 cells) were dislodged from plates with a 'rubber policeman' after being fixed for 15 min with 2% (vol/vol) paraformaldehyde and were washed with PBS containing 1% (vol/vol) FBS and 0.1% (wt/vol) sodium azide. Each well received 100 μl rabbit polyclonal anti–human annexin-1 or anti-AC2-26 (1 μg/ml; Phoenix Pharmaceuticals), followed by incubation for 1 h at 25 °C. After wells were washed twice, fluorescein isothiocyanate–conjugated goat anti-rabbit (diluted 1: 200; Zymed) was added for 45 min at 25 °C, then pellets were washed three time and then analyzed by flow cytometry. For analysis of total cell-associated annexin-1, cells were made permeable with PBS containing 1% FBS, 0.2% (wt/vol) saponin and 0.05% (wt/vol) sodium azide before being fixed for 10 min at 4 °C. For fluorescence microscopy, RAW 264.7 cells were cultured in 35-mm glass-bottomed microwell dishes at a density of 1.5×10^6 cells per well. Cells were then subjected to the experimental conditions, washed, and then incubated for 30 min with anti-Ac2-26 (5 μg/ml) and for 30 min with fluorescent goat anti-rabbit. After being washed, cells were examined by fluorescence microscopy.

Immunoblot analysis. Extracts from 5×10^5 cells were incubated for 1 h at 4 °C in buffer containing Triton X-100 (20 mM Tris, pH 7.5, 1% (vol/vol)

Triton X-100, 1% (vol/vol) glycerol, 137 mM NaCl, 2 mM EDTA, 25 mM β-glycerophosphate and protease inhibitor 'cocktail') and then centrifuged for 10 min at 4 °C and the supernatant was saved. Alternatively, cells were extracted for 5 min at 4 °C with 2 mM EDTA in PBS (1 µl per well). Protein was measured with the Bradford assay. Samples (10 µg) were fractionated by 12% PAGE and proteins were transferred to a nylon membrane at 4 °C. The membrane was blocked for 1 h with 5% (wt/vol) milk in 10 mM Tris HCl buffer, pH 8.0, 150 mM NaCl and 0.5% (vol/vol) Tween 20 and was probed with the appropriate primary antibodies. After three washes, blots were probed with goat polyclonal anti-rabbit for annexin-1 and goat polyclonal anti-mouse for actin. Enhanced chemiluminescence chemifluorescence reagent was added and blots were exposed to Kodak X film.

The human PAI2 probe was obtained from the J7 plasmid (American Type Culture Collection) by digestion with *Xba*I. A fragment 0.9 kb in length (nucleotides 790–1776) was purified by agarose gel electrophoresis and RNA was extracted (RNeasy Extract Total RNA kit; Qiagen). RNA (15 µg) was fractionated by electrophoresis through a 1.2% (vol/vol) formaldehyde gel and was transferred to a Hybond membrane (Hybond-N^+ RPN203; Amersham). The membrane was dried for 20 min at 80 °C, was soaked for 5 min in 2× 0.3 M sodium citrate buffer, pH 7.0, containing 0.3 M NaCl, and was prehybridized for 30 min at 65 °C in 10 ml Rapid Hybridization solution (Amersham). The probe was labeled with ^{32}P[dCTP] with a random-primer labeling kit (Stratagene) and was purified over a G50 column (Pharmacia) to exclude unbound radioactivity. Then, 100 µl salmon sperm DNA (2 mg/ml) was added to the probe, the solution was boiled for 5 min, and 5×10^7 c.p.m. of the probe was added to a roller bottle containing the blot, followed by hybridization for 2 h at 65 °C. Then the membrane was washed for 15 min at 25 °C with 2× SSC and then for 15 min at 65 °C with 0.1× SSC. The membrane was then exposed overnight at –80 °C to Kodak Biomax film.

Real-time PCR. Total RNA was isolated from macrophages with the RNeasy Kit and then was transcribed into cDNA with the Quantitect Reverse Transcription Kit according to the manufacturer's recommendations (Qiagen). The cDNA was denatured for 10 min at 95 °C. Specific DNA fragments were amplified with a Max3000p Stratagene cycler with 40 cycles of 15 s at 95 °C, 60 s at 60 °C and 30 s at 72 °C. The oligonucleotide primers were as follows: for human actin, 5′-AGTCCTGTGGCATTCACGAAACTA-3′ (forward) and 5′-ACTCCTGCTTG CTGATCCACATCT-3′ (reverse); and for PAI2, 5′-TCCTTTCCGTGTAAA CTCGGCTCA-3′ (forward) and 5′-GAAATTGGCCCGTCCCTTGTTGAA-3′ (reverse). The amount of amplified DNA fragments encoding PAI2 was normalized to that of fragments encoding actin. Results are presented as the 'fold difference' in gene expression.

Silencing of the gene encoding mouse annexin-1. Primers from the gene encoding mouse annexin-1 (Mouse GenBank accession number NM-010730) were used to design siRNAs (Dharmacon). Sequence consisting of residues 269–288 (TCATTGACATTCTTACCAA; targeted) and 321–339 (CCGC GTAGTTACAGGAGAA; nontargeted) with the loop sequence (TTCAAGAGA) and the *Hpa*1 and *Xho*1 cleavage sites was used to produce two short hairpin double-stranded RNA-1 primers. Construction of the vectors for silencing RAW 264.7 cells is described in the **Supplementary Methods** online.

Cell death and population analysis. BALB/c mice 6–8 weeks of age (Charles River Laboratories) were infected by tracheal instillation of H37Ra or H37Rv at a dose of 1×10^5 bacteria per mouse. Mice were lightly anesthetized with isoflurane, and 50 µl bacterial solution was pipetted into pharyngeal space while the tongue was extended to facilitate inhalation. Mice were killed 9 or 14 d after infection and cells were collected by BAL by flushing of the lungs three times with 1.5 ml PBS containing 0.2% (wt/vol) BSA and 0.2 mM EGTA. To maintain viability of cells in BAL fluid, the serum concentration was raised to 10% (vol/vol) immediately after cell recovery. Necrosis measured by staining of the cells for 15 min with propidium iodide (25 µg/ml; Molecular Probes), then 1% (vol/vol) paraformaldehyde was added and cell death was measured with an LSRII flow cytometer and FACSDiva software (BD Biosciences). For population analysis, cells in BAL fluid were stained with Pacific blue–anti-CD11b (M1/70), phycoerythrin–anti-CD11c (N418) and allophycocyanin–anti-F4/80 (BM8; all from eBiosciences), and phycoerythrin-indotricarbocyanine–anti-Gr-1 (RB6-8c5; BD Pharmingen). An LSRII flow cytometer (BD Biosciences Pharmingen) was used for flow cytometry and data were analyzed with FlowJo software (TreeStar). On the basis of four-color staining, resident alveolar macrophages were defined as $CD11b^{lo}CD11c^{hi}$, myeloid dendritic cells a were defined as $CD11b^{hi}CD11c^{hi}$, and granulocytes were defined as $Gr\text{-}1^+F4/80^-$.

Statistics. Data were analyzed with Microsoft Excel Statistical Software (Jandel) with the *t*-test for normally distributed data with equal variances. A *P* value of less than 0.05 was considered statistically significant.

Note: Supplementary information is available on the Nature Immunology website.

ACKNOWLEDGMENTS

We thank H.F. Rosenberg (National Institute of Allergy and Infectious Diseases) for mice with deletion of the gene encoding PAI2; E. Remold-O'Donnell and T. Vallerskog for discussions; and S. Remold for help with **Supplementary Figure 6**. Supported by US National Institutes of Health (AI50216 and HL064884).

AUTHOR CONTRIBUTIONS

H.G. did the *in vitro* work and contributed to the interpretation of experiments; J.L. did the *in vivo* mouse experimental work and analyzed the data; F.R. generated the PAI2 mutants; M.C. contributed to the experimental work and analyzed data; H.K. designed the *in vivo* mouse experiments, contributed to the interpretation of data, analyzed data and prepared parts of the manuscript; and H.G.R. planned the project, analyzed data and prepared the figures and the manuscript.

Published online at http://www.nature.com/natureimmunology/
Reprints and permissions information is available online at http://npg.nature.com/reprintsandpermissions/

1. Leemans, J.C. *et al.* Depletion of alveolar macrophages exerts protective effects in pulmonary tuberculosis in mice. *J. Immunol.* **166**, 4604–4611 (2001).
2. Vergne, I., Chua, J., Singh, S.B. & Deretic, V. Cell biology of *Mycobacterium tuberculosis* phagosome. *Annu. Rev. Cell Dev. Biol.* **20**, 367–394 (2004).
3. Keane, J. *et al.* Infection by *Mycobacterium tuberculosis* promotes human alveolar macrophage apoptosis. *Infect. Immun.* **65**, 298–304 (1997).
4. Riendeau, C.J. & Kornfeld, H. THP-1 cell apoptosis in response to Mycobacterial infection. *Infect. Immun.* **71**, 254–259 (2003).
5. Keane, J., Remold, H.G. & Kornfeld, H. Virulent *Mycobacterium tuberculosis* strains evade apoptosis of infected alveolar macrophages. *J. Immunol.* **164**, 2016–2020 (2000).
6. Spira, A. *et al.* Apoptosis genes in human alveolar macrophages infected with virulent or attenuated *Mycobacterium tuberculosis*: a pivotal role for tumor necrosis factor. *Am. J. Respir. Cell Mol. Biol.* **29**, 545–551 (2003).
7. Sly, L.M., Hingley-Wilson, S.M., Reiner, N.E. & McMaster, W.R. Survival of *Mycobacterium tuberculosis* in host macrophages involves resistance to apoptosis dependent upon induction of antiapoptotic Bcl-2 family member Mcl-1. *J. Immunol.* **170**, 430–437 (2003).
8. Balcewicz-Sablinska, M.K., Keane, J., Kornfeld, H. & Remold, H.G. Pathogenic *Mycobacterium tuberculosis* evades apoptosis of host macrophages by release of TNF-R2, resulting in inactivation of TNF-α. *J. Immunol.* **161**, 2636–2641 (1998).
9. Oddo, M. *et al.* Fas ligand-induced apoptosis of infected human alveolar macrophages reduces the viability of intracellular *Mycobacterium tuberculosis*. *J. Immunol.* **160**, 5448–5454 (1998).
10. Schaible, U.E. *et al.* Apoptosis facilitates antigen presentation to T lymphocytes through MHC-I and CD1 in tuberculosis. *Nat. Med.* **9**, 1039–1046 (2003).
11. Winau, F. *et al.* Apoptotic vesicles crossprime CD8 T cells and protect against tuberculosis. *Immunity* **24**, 105–117 (2006).
12. Park, J.S., Tamayo, M.H., Gonzalez-Juarrero, M., Orme, I.M. & Ordway, D.J. Virulent clinical isolates of *Mycobacterium tuberculosis* grow rapidly and induce cellular necrosis but minimal apoptosis in murine macrophages. *J. Leukoc. Biol.* **79**, 80–86 (2006).
13. Chen, M., Gan, H. & Remold, H.G. A mechanism of virulence: virulent *Mycobacterium tuberculosis* strain H37Rv, but not attenuated H37Ra, causes significant mitochondrial inner membrane disruption in macrophages leading to necrosis. *J. Immunol.* **176**, 3707–3716 (2006).
14. Lee, J., Remold, H.G., Ieong, M.H. & Kornfeld, H. Macrophage apoptosis in response to high intracellular burden of *Mycobacterium tuberculosis* is mediated by a novel caspase-independent pathway. *J. Immunol.* **176**, 4267–4274 (2006).
15. Robinson, N.A., Lapic, S., Welter, J.F. & Eckert, R.L. S100A11, S100A10, annexin I, desmosomal proteins, small proline-rich proteins, plasminogen activator inhibitor-2, and involucrin are components of the cornified envelope of cultured human epidermal keratinocytes. *J. Biol. Chem.* **272**, 12035–12046 (1997).
16. Fadok, V.A., Bratton, D.L. & Henson, P.M. Phagocyte receptors for apoptotic cells: recognition, uptake, and consequences. *J. Clin. Invest.* **108**, 957–962 (2001).

17. Fratazzi, C., Arbeit, R.D., Carini, C. & Remold, H.G. Programmed cell death of *Mycobacterium avium* serovar 4-infected human macrophages prevents mycobacteria from spreading and induces mycobacterial growth inhibition by freshly added, uninfected macrophages. *J. Immunol.* **158**, 4320–4327 (1997).
18. Pan, H. *et al. Ipr1* gene mediates innate immunity to tuberculosis. *Nature* **434**, 767–772 (2005).
19. Schlaepfer, D.D. & Haigler, H.T. Characterization of Ca^{2+}-dependent phospholipid binding and phosphorylation of lipocortin I. *J. Biol. Chem.* **262**, 6931–6937 (1987).
20. Ando, Y., Imamura, S., Owada, M.K., Kakunaga, T. & Kannagi, R. Cross-linking of lipocortin I and enhancement of its Ca^{2+} sensitivity by tissue transglutaminase. *Biochem. Biophys. Res. Commun.* **163**, 944–951 (1989).
21. Jensen, P.J., Wu, Q., Janowitz, P., Ando, Y. & Schechter, N.M. Plasminogen activator inhibitor type 2: an intracellular keratinocyte differentiation product that is incorporated into the cornified envelope. *Exp. Cell Res.* **217**, 65–71 (1995).
22. Traverso, V., Morris, J.F., Flowers, R.J. & Buckingham, J. Lipocortin 1 (annexin 1) in patches associated with the membrane of a lung adenocarcinoma cell line and in the cell cytoplasm. *J. Cell Sci.* **111**, 1405–1418 (1998).
23. Gerke, V., Creutz, C.E. & Moss, S.E. Annexins: linking Ca^{2+} signalling to membrane dynamics. *Nat. Rev. Mol. Cell Biol.* **6**, 449–461 (2005).
24. Kaufmann, S.H. & Earnshaw, W.C. Induction of apoptosis by cancer chemotherapy. *Exp. Cell Res.* **256**, 42–49 (2000).
25. Siefring, G.E. Jr., Apostol, A.B., Velasco, P.T. & Lorand, L. Enzymatic basis for the Ca^{2+}-induced cross-linking of membrane proteins in intact human erythrocytes. *Biochemistry* **17**, 2598–2604 (1978).
26. Ando, Y., Imamura, S., Owada, M.K. & Kannagi, R. Calcium-induced intracellular cross-linking of lipocortin I by tissue transglutaminase in A431 cells. Augmentation by membrane phospholipids. *J. Biol. Chem.* **266**, 1101–1108 (1991).
27. Oling, F., Bergsma-Schutter, W. & Brisson, A. Trimers, dimers of trimers, and trimers of trimers are common building blocks of annexin a5 two-dimensional crystals. *J. Struct. Biol.* **133**, 55–63 (2001).
28. Dickinson, J.L., Bates, E.J., Ferrante, A. & Antalis, T.M. Plasminogen activator inhibitor type 2 inhibits tumor necrosis factor α-induced apoptosis. Evidence for an alternate biological function. *J. Biol. Chem.* **270**, 27894–27904 (1995).
29. Gan, H., Newman, G.W. & Remold, H.G. Plasminogen activator inhibitor type 2 prevents programmed cell death of human macrophages infected with *Mycobacterium avium*, serovar 4. *J. Immunol.* **155**, 1304–1315 (1995).
30. Costelloe, E.O., Stacey, K.J., Antalis, T.M. & Hume, D.A. Regulation of the plasminogen activator inhibitor-2 (PAI-2) gene in murine macrophages. Demonstration of a novel pattern of responsiveness to bacterial endotoxin. *J. Leukoc. Biol.* **66**, 172–182 (1999).
31. Schwartz, B.S. & Bradshaw, J.D. Regulation of plasminogen activator inhibitor mRNA levels in lipopolysaccharide-stimulated human monocytes. *J. Biol. Chem.* **267**, 7089–7094 (1992).
32. Levy, B.D., Clish, C.B., Schmidt, B., Gronert, K. & Serhan, C.N. Lipid mediator class switching during acute inflammation signals in resolution. *Nat. Immunol.* **2**, 612–619 (2001).
33. Bafica, A. *et al.* Host control of *Mycobacterium tuberculosis* is regulated by lipoxygenase-dependent lipoxin production. *J. Clin. Invest.* **115**, 1601–1606 (2005).
34. Oliani, S.M., Paul-Clark, M.J., Christian, H.C., Flower, R.J. & Perretti, M. Neutrophil interaction with inflamed postcapillary venule endothelium alters annexin 1 expression. *Am. J. Pathol.* **158**, 603–615 (2001).
35. Jensen, P.H. *et al.* A unique interhelical insertion in plasminogen activator inhibitor-2 contains three glutamines, Gln83, Gln84, Gln86, essential for transglutaminase-mediated cross-linking. *J. Biol. Chem.* **269**, 15394–15398 (1994).
36. Jensen, P.H., Lorand, L., Ebbesen, P. & Gliemann, J. Type-2 plasminogen-activator inhibitor is a substrate for trophoblast transglutaminase and factor XIIIa. Transglutaminase-catalyzed cross-linking to cellular and extracellular structures. *Eur. J. Biochem.* **214**, 141–146 (1993).
37. Dickinson, J.L., Norris, B.J., Jensen, P.H. & Antalis, T.M. The C-D interhelical domain of the serpin plasminogen activator inhibitor-type 2 is required for protection from TNF-α induced apoptosis. *Cell Death Differ.* **5**, 163–171 (1998).
38. Silverman, G.A. *et al.* Human clade B serpins (ov-serpins) belong to a cohort of evolutionarily dispersed intracellular proteinase inhibitor clades that protect cells from promiscuous proteolysis. *Cell. Mol. Life Sci.* **61**, 301–325 (2004).
39. Barber, G.N. Host defense, viruses and apoptosis. *Cell Death Differ.* **8**, 113–126 (2001).
40. Keane, J., Shurtleff, B. & Kornfeld, H. TNF-dependent BALB/c murine macrophage apoptosis following *Mycobacterium tuberculosis* infection inhibits bacillary growth in an IFN-γ independent manner. *Tuberculosis (Edinb.)* **82**, 55–61 (2002).
41. Ciaramella, A. *et al.* Induction of apoptosis and release of interleukin-1 beta by cell wall-associated 19-kDa lipoprotein during the course of mycobacterial infection. *J. Infect. Dis.* **190**, 1167–1176 (2004).
42. Lopez, M. *et al.* The 19-kDa *Mycobacterium tuberculosis* protein induces macrophage apoptosis through Toll-like receptor-2. *J. Immunol.* **170**, 2409–2416 (2003).
43. Worku, S. & Hoft, D.F. Differential effects of control and antigen-specific T cells on intracellular mycobacterial growth. *Infect. Immun.* **71**, 1763–1773 (2003).
44. Wolf, A.J. *et al. Mycobacterium tuberculosis* infects dendritic cells with high frequency and impairs their function in vivo. *J. Immunol.* **179**, 2509–2519 (2007).
45. Li, M. *et al.* An essential role of the NF-κB/Toll like receptor pathways In induction of inflammatory and tissue-repair gene expression by necrotic cells. *J. Immunol.* **166**, 7128–7138 (2001).
46. Arur, S. *et al.* Annexin I is an endogenous ligand that mediates apoptotic cell engulfment. *Dev. Cell* **4**, 587–598 (2003).
47. Knight, R.L., Hand, D., Piacentini, M. & Griffin, M. Characterization of the transglutaminase-mediated large molecular weight polymer from rat liver; its relationship to apoptosis. *Eur. J. Cell Biol.* **60**, 210–216 (1993).
48. Steinert, P.M. & Marekov, L.N. The proteins elafin, filaggrin, keratin intermediate filaments, loricrin, and small proline-rich proteins 1 and 2 are isodipeptide cross-linked components of the human epidermal cornified cell envelope. *J. Biol. Chem.* **270**, 17702–17711 (1995).
49. Levitt, M.L., Gazdar, A.F., Oie, H.K., Schuller, H. & Thacher, S.M. Cross-linked envelope-related markers for squamous differentiation in human lung cancer cell lines. *Cancer Res.* **50**, 120–128 (1990).
50. Grenard, P. *et al.* Transglutaminase-mediated cross-linking is involved in the stabilization of extracellular matrix in human liver fibrosis. *J. Hepatol.* **35**, 367–375 (2001).
51. Lathem, W.W., Price, P.A., Miller, V. & Goldman, W. E. A plasminogen-activating protease specifically controls the development of primary pneumonic plague. *Science* **315**, 509–513 (2007).
52. Kruithof, E.K., Baker, M.S. & Bunn, C.L. Biological and clinical aspects of plasminogen activator inhibitor type 2. *Blood* **86**, 4007–4024 (1995).
53. von, H.G., Liljestrom, P., Mikus, P., Andersson, H. & Ny, T. The efficiency of the uncleaved secretion signal in the plasminogen activator inhibitor type 2 protein can be enhanced by point mutations that increase its hydrophobicity. *J. Biol. Chem.* **266**, 15240–15243 (1991).
54. Kruithof, E.K., Vassalli, J.D., Schleuning, W.D., Mattaliano, R.J. & Bachmann, F. Purification and characterization of a plasminogen activator inhibitor from the histiocytic lymphoma cell line U-937. *J. Biol. Chem.* **261**, 11207–11213 (1986).
55. Vassalli, J.D., Dayer, J.M., Wohlwend, A. & Belin, D. Concomitant secretion of prourokinase and of a plasminogen activator-specific inhibitor by cultured human monocytes-macrophages. *J. Exp. Med.* **159**, 1653–1668 (1984).
56. Chan, F.K. *et al.* A role for tumor necrosis factor receptor-2 and receptor-interacting protein in programmed necrosis and antiviral responses. *J. Biol. Chem.* **278**, 51613–51621 (2003).
57. Kroemer, G., Dallaporta, B. & Resche-Rigon, M. The mitochondrial death/life regulator in apoptosis and necrosis. *Annu. Rev. Physiol.* **60**, 619–642 (1998).
58. Dougherty, K.M. *et al.* The plasminogen activator inhibitor-2 gene is not required for normal murine development or survival. *Proc. Natl. Acad. Sci.* **96**, 686–691 (1999).
59. Mosmann, T. Rapid colorimetric assay for cellular growth and survival: application to proliferation and cytotoxicity assays. *J. Immunol. Methods* **65**, 55–63 (1983).